BIOLOGY OF REPRODUCTION **82,** 246–256 (2010)
Published online before print 30 September 2009.
DOI 10.1095/biolreprod.109.077925

Subfertility Caused by Altered Follicular Development and Oocyte Growth in Female Mice Lacking *PKBalpha/Akt1*[1]

Caitlin Brown, Jessica LaRocca, Jodie Pietruska, Melissa Ota, Linnea Anderson, Stuart Duncan Smith, Paula Weston, Teresa Rasoulpour, and Mary L. Hixon[2]

Department of Pathology and Laboratory Medicine, Brown University, Providence, Rhode Island

ABSTRACT

Mammalian females are endowed with a finite number of primordial follicles at birth. Immediately following formation of the primordial follicle pool, cohorts of follicles are either culled from the ovary or are recruited to grow until the primordial follicle population is depleted. The majority of ovarian follicles, including the oocytes, undergo atresia through apoptotic cell death. As *PKBalpha/Akt1* is known to regulate apoptosis, we asked whether *Akt1* functioned in the regulation of folliculogenesis in the ovary. *Akt1*$^{-/-}$ females display reduced fertility and abnormal estrous cyclicity. At Postnatal Day (PND) 25, *Akt1*$^{-/-}$ ovaries possessed a reduced number of growing antral follicles, significantly larger primary and secondary oocytes, and an increase in the number of degenerate oocytes. By PND90, there was a significant decrease in the number of primordial follicles in *Akt1*$^{-/-}$ ovaries relative to *Akt1*$^{+/+}$. In vivo granulosa cell proliferation was reduced, as were expression levels of *Kitl* and *Bcl2l1*, two factors associated with granulosa cell proliferation/survival. No compensation was observed by *Akt2* or *Akt3* at the mRNA/protein level. Significantly higher serum LH and trends for lower FSH and higher inhibin A and lower inhibin B relative to *Akt1*$^{+/+}$ females were observed in *Akt1*$^{-/-}$ females. Exposure to exogenous gonadotropins resulted in an increase in the number of secondary follicles in *Akt1*$^{-/-}$ ovaries, but few mature follicles. Collectively, our results suggest that *PKBalpha/Akt1* plays an instrumental role in the regulation of the growth and maturation of the ovary, and that the loss of *PKBalpha/Akt1* results in premature ovarian failure.

granulosa cells, kinases, ovary

INTRODUCTION

In mammals, the follicle is the basic unit of the ovary. Each follicle contains an oocyte that is surrounded by granulosa cells [1]. The vast majority of follicles remain as dormant primordial follicles containing immature oocytes. However, a limited number of primordial follicles are recruited from the resting follicle reserve into the growing follicle pool. The activation of primordial follicles is a highly regulated process, and when activation of the primordial follicle pool ceases, the reproductive life of the female ends. This exhaustion of the primordial follicle pool usually occurs at menopause. Hence, the duration of fertility of a female is determined by the initial size of her primordial follicle pool and by the rate of its activation and subsequent depletion [2]. The maturation of ovarian follicles is a complex process involving intra- and extraovarian signaling. While the components and mechanisms of the intraovarian signaling are largely unknown, the integration of FSH and LH in the process is well documented [3, 4]. The function of FSH is to stimulate ovarian follicle maturation. It achieves this by initiating granulosa cell growth and promoting the transition from primary follicles to secondary and Graafian follicles in preparation for ovulation. The main function of LH occurs at the peak of estrus. LH is released in a pulsatile manner at low concentrations during folliculogenesis, and spikes to promote ovulation [4]. In contrast, the primordial to primary follicle transition is independent of these hormones [5].

Recent evidence implicates the PTEN/PIK3/PDK1/AKT signaling pathway in the regulation of primordial follicle activation [6]. Mice deleted for the oocyte-specific expression of PTEN, the phosphatase and tensin homolog tumor suppressor gene, exhibit premature ovarian failure (POF) due to the rapid activation and subsequent depletion of the primordial follicle pool [6]. In addition to PTEN-deficient mice, female mice deficient for 3-phosphoinositide-dependent protein kinase (PDK) 1 also exhibit female infertility, with significant primordial follicle loss around the onset of sexual maturity causing POF during early adulthood [7]. Another downstream target of *Akt1*, *Foxo3a* null mice exhibit increased primordial follicle activation resulting in complete follicle loss by 15 wk of age [8]. Therefore, the evidence indicates that the PTEN/PIK3/PDK1/AKT signaling pathway is a key pathway in the regulation of female fertility.

The phosphoinositide 3-kinase signaling pathway is a critical regulator of cellular processes, such as cell growth, proliferation, differentiation, and survival. These actions are achieved by phosphorylation and the subsequent activation of effector proteins, one of which is the prosurvival protein kinase, AKT. AKT and PDK1 are recruited to the membrane via their pleckstrin homology domains, and PDK1 subsequently phosphorylates the kinase domain of AKT1 at Thr308, which is required for AKT activation. A second serine residue, Ser473, is contained in the regulatory domain, and must be phosphorylated in order for AKT to exhibit full kinase activity [9].

Targeted disruption of the *PKB*/*Akt* gene family has provided valuable insights into the role of these proteins in both development and disease. Homozygous disruption of *Akt1* results in growth retardation and increased apoptosis in several tissue types [10, 11]. Mice that harbor a deletion of the *Akt*2 gene demonstrate insulin resistance and a diabetes mellitus-like syndrome [12, 13]. Homozygous deletion of both *Akt1* and *Akt2* in mice leads to dwarfism, impaired skin development,

[1]Supported by the Innovations in Women's Health Seed Grant Program with funds from Women and Infants Hospital of Rhode Island and The Warren Alpert School of Medicine at Brown University and ES015704 to M.L.H.
[2]Correspondence: Mary L. Hixon, GE505, Department of Pathology and Laboratory Medicine, Brown University; Providence, RI 02912. FAX: 401 863 9008; e-mail: mary_hixon@brown.edu

Received: 31 March 2009.
First decision: 21 April 2009.
Accepted: 17 September 2009.

eISSN: 1529-7268 http://www.biolreprod.org
ISSN: 0006-3363

skeletal muscle atrophy, delayed bone development, and impeded adipogenesis [14]; in addition, dosage-dependent effects are observed in the thymus and skin, and in the cardiovascular and nervous systems, in mice with homozygous disruptions in both *Akt1* and *Akt3* [15]. In addition, *Akt3* has been shown to be instrumental in the attainment of normal brain size [16, 17].

Despite intense research on the biological functions of the PKB/*Akt* gene family, relatively little is known about its role in female reproductive physiology. $Akt1^{-/-}$ males are fertile, but are more sensitive to both genotoxic and nongenotoxic insults [18, 19]. $Akt1^{-/-}$ female mice have been reported to have reduced fertility, whereas *Akt*3 females are reported to have normal fertility [20]. It is unknown as to whether *Akt2* female mice have reduced fertility. In the ovary, *Akt1* has been localized in porcine granulosa cells of primordial follicles and in the basal layers of the granulosa cells of preantral and antral follicles, but not in atretic follicles or corpora lutea [21]. In rodents, *Akt1* is found in both granulosa cells of the ovary and in oocytes [22, 23]. In the human ovary, *Akt1* expression is found in oocytes, in granulosa cells, and in the thecal cells of primordial follicles, in follicles at each growing stage, and in the luteal cells [24].

In the present study, we investigate the effect of *Akt1* deletion on female reproductive physiology in the mouse. We found that $Akt1^{-/-}$ females display reduced fertility, a delay in the onset of estrus, an increase in maternal age at first litter, and a reduction in average litter size. At Postnatal Day (PND) 25, $Akt1^{-/-}$ ovaries contain a significantly reduced number of growing early antral and antral follicles. The oocytes of primary follicles of $Akt1^{-/-}$ females are larger than $Akt1^{+/+}$ animals with some follicles exhibiting multiple oocytes, suggesting a defect in cyst breakdown. $Akt1^{-/-}$ ovaries possessed a reduced number of mature follicles, decreased in vivo granulosa cell proliferation in secondary follicles, and an increase in the number of degenerate oocytes. By PND90, there was a significant decrease in the number of primordial follicles in $Akt1^{-/-}$ females relative to their $Akt1^{+/+}$ counterparts. At the molecular level, decreased expression of the cell cycle regulator, *Ccnd3*, and a trend for decreased *Ccnd1* was observed. The KITL survival factor, which is expressed primarily by the granulosa cells, was significantly reduced in the $Akt1^{-/-}$ ovary, and decreased expression of the antiapoptoptic factor, *Bcl2l1*, was also observed. Taken together, our data reveal that *Akt1* deletion produces changes in the ovary and oocyte, which lead to infertility and the onset of POF.

MATERIALS AND METHODS

Mice

Akt1 heterozygous breeding pairs in a C57BL/6 background were obtained from the laboratory of Dr. Morris Birnbaum (University of Pennsylvania, Philadelphia, PA). Heterozygous pairs were mated to obtain $Akt1^{+/+}$, $Akt1^{+/-}$, and $Akt1^{-/-}$ females for experimental procedures. The frequency of obtaining $Akt1^{-/-}$ mice is approximately 17.3 percent, which is less than the expected Mendelian frequency of 25%. Experiments were conducted at PNDs 25, 50, 56, and 90. The animal room climate was kept at a constant temperature (23.3 ± 2°C) at 30%–70% humidity, with an alternating 12L:12D cycle. All procedures involving animals were performed in accordance with the guidelines of the Institutional Animal Care and Use Committee of Brown University in compliance with the guidelines established by the National Institutes of Health.

Primers

For genotyping by PCR, the following primers were used in a single reaction: 853, 5′-GTGGATGTGGAATGTGTGCGAG-3′; 854, 5′-GCTCAGTCAGTGAGGCCAGACC-3′; 855, 5′-CACCCCACAAGCTCT-TCTTCCA-3′. The PCR was run with an initial denaturing step of 94°C for 5 min, 39 cycles of 94°C for 30 sec, 63°C for 30 sec, 72°C for 45 sec, followed by a final extension at 72°C for 5 min. For PCR genotyping of progeny, the wild-type and targeted bands were 310 and 194 bp, respectively.

Fertility Analysis

To evaluate the reproductive performance of $Akt1^{-/-}$ mice, seven individually housed $Akt1^{-/-}$ females were bred to $Akt1^{+/+}$ males of proven fertility. $Akt1^{+/+}$ females were used as controls. The females were introduced to the males at 7 to 8 wk of age, and the number of litters and the number of pups were recorded over a minimum 6-mo period.

Assessment of Pubertal Onset and Estrous Cyclicity

To assess the onset of puberty in juvenile females, mice were observed daily for signs of vaginal opening. The onset of estrus was also monitored by daily vaginal lavage of females in the morning, for a period of at least 1 mo after vaginal opening based on vaginal cytology, according to the classification of Pedersen [25].

Classification of the Estrous Cycle and Tissue Collection

To examine the influence of genotype on the length of the estrous cycle, vaginal smears from wild-type and *Akt1*-deficient female mice at 12 wk of age were monitored daily between 0800 and 1000 h. The mouse's tail was raised and a 20-μl pipette tip filled with sterile PBS1X was inserted into the vagina and washed up and down. When the tip was removed, it was dropped onto a microscope slide. The smears were classified into one of four phases of estrus: elongated nucleated epithelium indicated proestrus; large cornified epithelial cells were exclusively found in estrus; metestrus was marked by a thick smear composed of equal numbers of nucleated epithelial cells and leukocytes; and a smear consisting almost exclusively of leukocytes depicted diestrus [26]. Each cycle length was determined as the length of time between two consecutive occurrences of estrus. After the mice had progressed through at least three consecutive estrous cycles, the length of the estrous cycle and the number of days spent at each stage of the cycle were evaluated.

Ovarian Histology

To determine whether lack of *Akt1* influences ovarian development, ovaries from a minimum of three mice per genotype were collected and examined at PNDs 25 and 90. Both ovaries were removed, cleaned of extraneous tissue, weighed, and fixed in Bouins. Tissues were then embedded in paraffin and serial sections (7-μm thick) of ovaries were stained with periodic acid-Schiff (PAS).

Assessment of Follicle Development

In approximately every 10th ovarian section, the numbers of primordial, primary, early antral, and healthy antral follicles were counted. Only follicles containing an oocyte with a visible nucleus were counted to avoid double counting, and all counting was done without the knowledge of genotype. Follicles were counted as primordial if they contained an oocyte surrounded by flattened granulosa cells, or a mixture of less than seven flattened and cuboidal granulosa cells. Follicles were counted as primary if they contained an oocyte surrounded by a single layer of seven or more cuboidal granulosa cells. Secondary follicles were those containing an oocyte surrounded by two or more complete layers of granulosa cells. Early antral follicles were those with more than four complete layers of granulosa cells and an antrum <20 μm in diameter. Antral follicles were considered as those that had a visible antrum without a stalk. Graafian follicles were those with a large antrum, cumulous oophorus, and a corona radiata. Antral follicles were considered to be healthy if they had an intact oocyte and $<10\%$ pyknotic granulosa cells. Antral follicles were considered to be atretic if there were more than 10% pyknotic granulosa cells.

Superovulation

Female mice at 24–26 days of age were injected i.p. with 5.0 IU of ECG followed by 5.0 IU of hCG i.p. 48 h later. Oviducts and ovaries were excised from mice 18 h after hCG administration, and were fixed in 10% neutral buffered formalin. Tissues were then embedded in paraffin and serial sections (7-μm thick) of ovaries were stained with PAS. For analysis of the number of ovarian follicles, every sixth section was mounted and stained with hematoxylin and eosin.

TABLE 1. Effect of *Akt1* null mutation on female fertility.[a]

Genotype	N	Litter	Total pups	Pups/litter	Litters/month	Days to vaginal opening	Age at first estrous cycle (days)	Age at first litter (days)
$Akt1^{+/+}$	5	18	103	5.81 ± 0.5	0.644 ± 0.1	33 ± 1.5 (N = 4)	39.8 ± 1.1 (N = 3)	56 ± 5
$Akt1^{-/-}$	8	5	20	3.56 ± 0.8*	0.112 ± 0.1*	33.2 ± 1.4 (N = 10)	44.8 ± 0.6* (N = 3)	100 ± 7.2*

[a] Values represent the mean ± SEM; statistical analyses were conducted using Student *t*-test ($P < 0.05$).
* Significant differences observed between $Akt1^{+/+}$ and $Akt1^{-/-}$ animals.

Primary Oocyte Diameter

Ovaries from mice at PND25 were examined (n = 3–4 ovaries per genotype). A total of 87 and 118 primary follicles were measured from $Akt1^{+/+}$ and $Akt1^{-/-}$ mice, respectively. Follicles were counted as primary if they contained an oocyte surrounded by a single layer of seven or more cuboidal granulosa cells. To prevent counting the same oocyte twice, oocytes were only measured when there was a visible nucleolus. Measurements were then averaged and expressed as the diameter of the oocyte.

Secondary Oocyte Diameter

Ovaries from mice at PND25 were examined (n = 3–4 ovaries per genotype). A total of 55 and 66 secondary follicles were measured from $Akt1^{+/+}$ and $Akt1^{-/-}$ mice, respectively. Follicles were counted as secondary if they contained an oocyte surrounded by two or more complete layers of granulosa cells and no visible antrum formation. To prevent counting the same oocyte twice, oocytes were only measured when there was a visible nucleolus. Measurements were then averaged and expressed as the diameter of the oocyte.

Measurements of Hormone Levels

To measure serum FSH, LH, inhibin A and B, progesterone, and estradiol levels, blood samples were collected by cardiac puncture from randomly cycling $Akt1^{+/+}$ and $Akt1^{-/-}$ female mice at specific ages. The serum was stored at −80°C until assayed. FSH, LH, inhibin A and B, progesterone, and estradiol levels were assayed by the University of Virginia Ligand Core Facility as described (http://www.healthsystem.virginia.edu/internet/crr/ligand.cfm; Specialized Cooperative Center Program in Reproductive Research, National Institute of Child Health and Human Development/National Institutes of Health U54 HD28934).

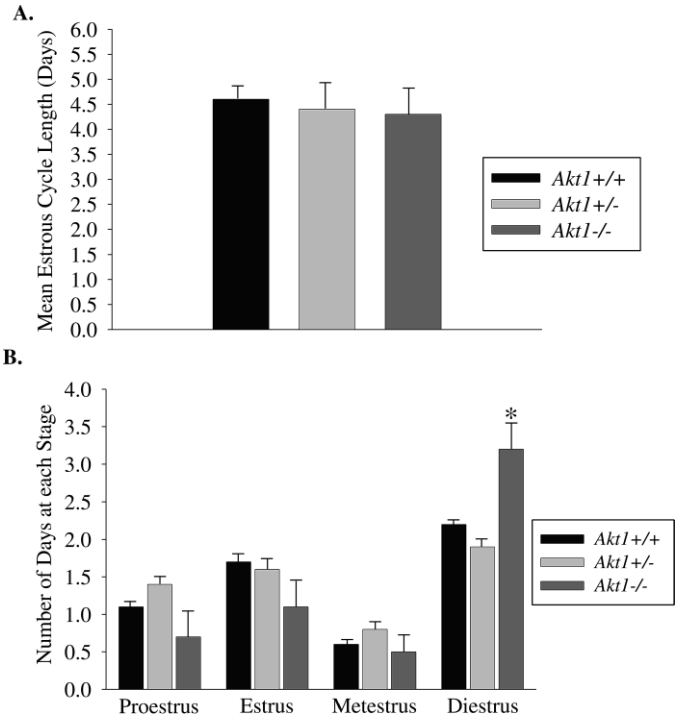

FIG. 1. *Akt*1 influences estrus cycle phase in female mice at PND90. **A**) Graph depicts the mean estrous cycle length of $Akt1^{+/+}$ (black bar), $Akt1^{+/-}$ (light gray bar), and $Akt1^{-/-}$ (dark gray bar) female mice. **B**) Graph shows the average number of days that each genotype stayed within individual stages of the estrous cycle ($P < 0.05$). Asterisk indicates significant differences observed between $Akt1^{+/+}$ and $Akt1^{-/-}$ animals.

Bromodeoxyuridine Incorporation

Assessment of granulosa cell proliferation by bromodeoxyuridine (BrdU) incorporation was performed. Hormonally primed mice (5 IU eCG) were injected intraperitoneally with 1 μg/g BrdU and killed after 1 h. The ovaries were dissected, fixed in formalin, and 7-μm serial sections were generated. Primary monoclonal anti-BrdU antibody (Dako) was used at a 1:100 dilution. After counterstaining with methyl green, the number of BrdU-positive cells per follicle was determined for comparison in a minimum of five follicles per experimental animal. Secondary follicles were analyzed in the eCG-treated groups.

Immunohistochemistry

Immunohistochemistry was performed on formalin-fixed, paraffin-embedded 7-μm sections using the VectaStain Elite Avidin-Biotin Complex Kit, as directed by the manufacturer (Vector Labs, Burlingame, CA). Sections were probed with primary antibodies against CCND1 and CCND3 both from Cell Signaling (Beverly, MA) and CCND2 from Santa Cruz Research (Santa Cruz, CA). Sections were visualized using a 3,3′-diaminobenzidine peroxidase Substrate Kit (Vector Labs). Digital images were captured using the Aperio Scanscope Imaging System (Vista, CA).

Western Blot Analysis

Ovaries were lysed by homogenization in cold lysis buffer (50 mM Tris 8.0, 250 mM NaCl, 1% NP-40, 0.1% SDS, 5 mM EDTA, 2 mM Na_3VO_4, 10 mM $Na_2P_2O_7$, 10 mM NaF) supplemented with 1 mM PMSF and 40 μl/ml Complete Protease Inhibitor Cocktail (Roche, Indianapolis, IN). Lysates were incubated on ice for 20 min with frequent vortexing and cleared by centrifugation (10 000 rpm, 10 min, 4°C). Protein concentrations were determined using the DC Protein Assay (Bio-Rad, Hercules, CA). Total protein (50 μg) was subjected to SDS-PAGE and transferred onto Immobilon-P polyvinylidene fluoride (Millipore, Billerica, MA). Membranes were blocked for 60 min at room temperature in 5% nonfat milk/Tris-buffered saline/0.1% Tween (TBST). Membranes were incubated for 2 h at room temperature, then overnight at 4°C in the following antibodies: phospho-AKT (Thr308) (#9275, 1:500 in 5% milk/TBST), phospho-AKT (Ser473) (#9271, 1:1000 in 5% milk/TBST), AKT1 (#2967, 1:1000 in 5% milk/TBST), AKT2 (#2964, 1:1000 in 5% milk/TBST), AKT3 (#4059, 1:1000 in 5% milk/TBST). All antibodies were obtained from Cell Signaling Technology (Danvers, MA). Membranes were washed three times (5 min/wash) in TBST, and incubated for 60 min at room temperature in horseradish peroxidase-conjugated goat anti-rabbit IgG or goat anti-mouse IgG (Cell Signaling), diluted 1:2000 in 5% milk/TBST. Membranes were washed three times (5 min/wash) in TBST, and once in TBS prior to visualization using enhanced chemiluminescence (GE Healthcare, Piscataway, NJ).

Quantitative RT-PCR

Total RNA (1 μg) was DNase-I (Invitrogen, Carlsbad, CA) treated and reverse transcribed using iScript cDNA Synthesis Kit (Bio-Rad) according to the manufacturer's protocols, and the cDNA templates were amplified with each of the primer pairs in independent sets of PCR using iQ SYBR Green Supermix (Bio-Rad) on an iCycler iQ Multicolor Real-Time PCR Detection System (Bio-Rad). The concentration of Mg^{2+} and the linear range of amplification of cDNAs with each primer pair first were optimized, and cDNAs subsequently were tested. Each sample was run in triplicate, and mRNA levels were analyzed relative to hypoxanthine phosphoribosyltransferase.

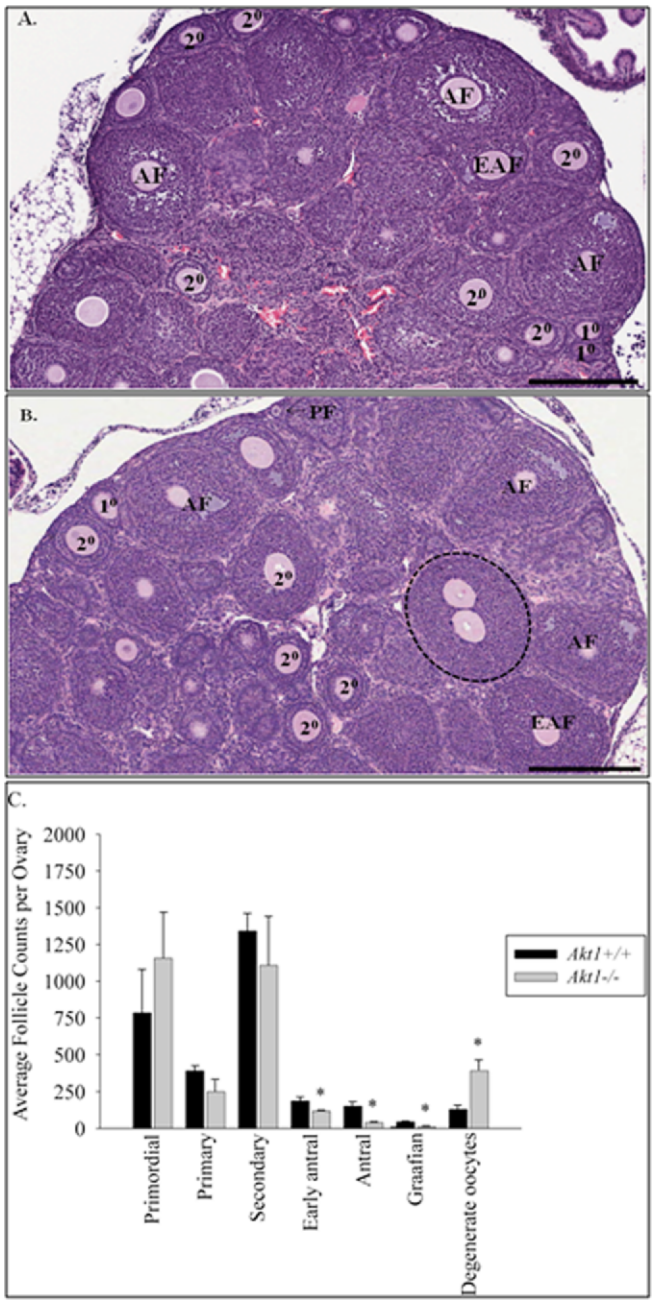

FIG. 2. Effect of *Akt1* null mutation on ovarian follicle development at PND25. **A**) $Akt1^{+/+}$ ovary at PND25. **B**) $Akt1^{-/-}$ ovary at PND25. **C**) Follicle counts of $Akt1^{+/+}$ and $Akt1^{-/-}$ females at PND25 ($n = 3$). The number of primordial (PF), primary(1^0), secondary (2^0), early antral (EAF), antral (AF), and mature Graafian follicles (GF) were determined in $Akt1^{+/+}$ and $Akt1^{-/-}$ at PND25. Ovaries were serially sectioned, every 10th section was counted, and the total follicle numbers were determined. The total numbers of primordial, primary, secondary, early antral, antral, and mature follicles were multiplied by a factor of 10 to obtain an estimate of the total number of follicles per ovary. These data represent the mean ± SEM of combined results from the analysis of three mice per age group ($P < 0.05$). Asterisks indicate significant differences in follicle number observed between $Akt1^{+/+}$ and $Akt1^{-/-}$ animals; bar = 200 μm.

Mouse-specific primers were designed using Molecular Beacon Design 4.0 Software (Bio-Rad). Specific primer sequences for each gene for quantitative RT-PCR were as follows: *Kitl* = forward, 5′-ACAGCAGTAGCAGTAATAGG-3′ and *Kitl* = reverse, 5′-GACTTGACTGTTTCTTCTTCC-3′; *Bcl2l1* = forward, 5′-CCGCTGTGTCTCTGGGTCTC-3′ and *Bcl2l1* = reverse, 5′-GGTTCTGGTCCTTGTCTCATTATCC-3′; *Ccnd1* = forward, 5′-ATGTTGT TACCAGAAGAGGAAG-3′ and *Ccnd1* = reverse, 5′-TCAGATAGAAAG

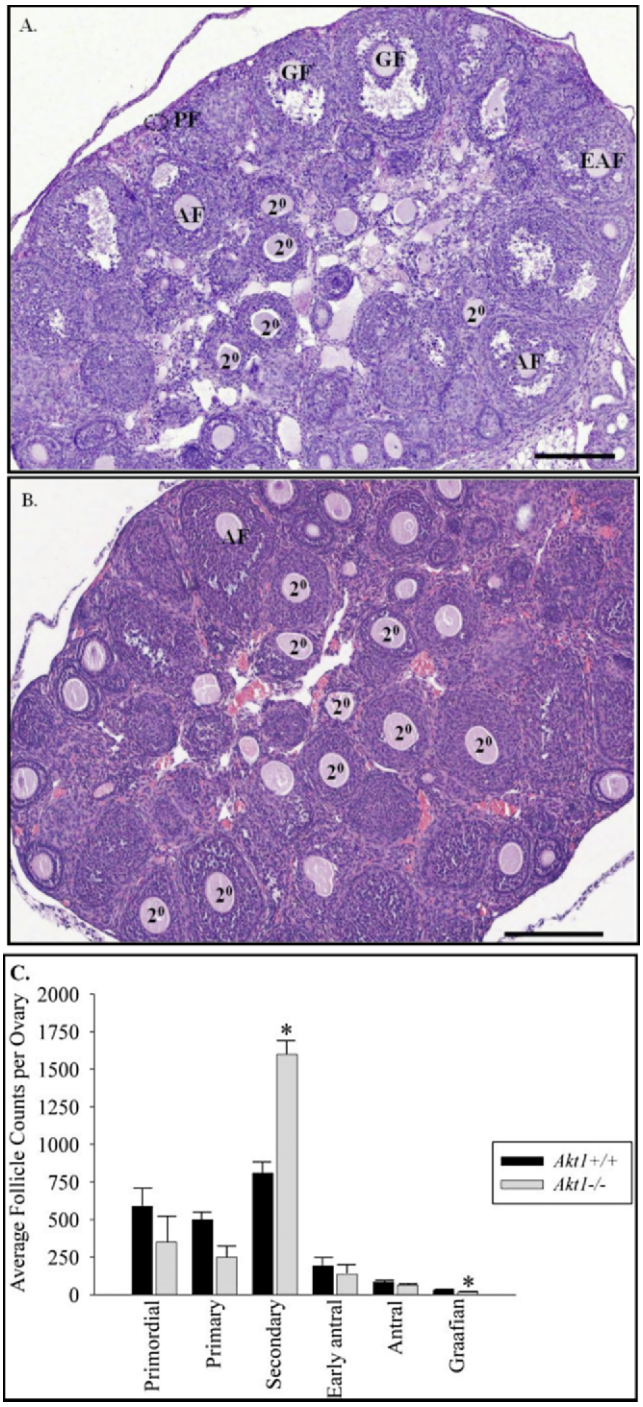

FIG. 3. Responsiveness of *Akt1* null mutant mice to exogenous gonadotropins at PND25. Histology of ovaries from $Akt1^{+/+}$ (**A**) and $Akt1^{-/-}$ (**B**) animals exposed to exogenous gonadotropins. Female mice at 24–26 days of age were injected i.p. with 5.0 IU of ECG followed by 5.0 IU of hCG i.p. 48 h later. Oviducts and ovaries were excised from mice 18 h after hCG. **C**) The number of primordial (PF), primary (1^0), secondary (2^0), early antral (EAF), antral (AF), and mature Graafian follicles (GF) were determined in $Akt1^{+/+}$ and $Akt1^{-/-}$ at PND25 following exposure to exogenous gonadotropins. Ovaries were serially sectioned, every sixth section was counted, and the total follicle numbers were determined. The total numbers of primordial, primary, secondary, early antral, antral, and mature follicles were multiplied by a factor of six to obtain an estimate of the total number of follicles per ovary. These data represent the mean ± SEM of combined results from the analysis of three mice per age group ($P < 0.05$). Asterisks indicate significant differences in follicle number observed between $Akt1^{+/+}$ and $Akt1^{-/-}$ animals; bar = 200 μm.

TABLE 2. Comparison of *Akt1*$^{+/+}$ and *Akt1*$^{-/-}$ female body and ovarian weights at PND25, PND56, and PND90.[a]

Genotype	Body weight (g)	Combined ovarian weight (mg)	Ovary weight:BW ratio (mg/g)
PND25			
Akt1$^{+/+}$	11.0 ± 1.5	8.4 ± 1.1	0.76
Akt1$^{-/-}$	7.0 ± 1.2*	6.1 ± 0.5*	0.87
PND56			
Akt1$^{+/+}$	18.7 ± 0.8 (N = 6)	11.5 ± 1.3 (N = 6)	0.61
Akt1$^{-/-}$	14.7 ± 0.4* (N = 26)	10.8 ± 0.8* (N = 20)	0.73
PND90			
Akt1$^{+/+}$	21.1 ± 0.4 (N = 15)	17.4 ± 0.6 (N = 15)	0.82
Akt1$^{-/-}$	18.6 ± 0.3* (N = 21)	13.8 ± 0.6* (N = 20)	0.74

[a] Values represent the mean ± SEM; statistical analyses were conducted using one-way ANOVA ($P < 0.05$).
* Significant differences observed between *Akt1*$^{+/+}$ and *Akt1*$^{-/-}$ animals at specific postnatal ages.

GAGAAAGATTAAGG-3′; *Ccnd2* = forward, 5′-TGGCAGA CAGTTAGGAGAC-3′ and *Ccnd2* = reverse, 5′-AGCACCAACCAGACT CAG-3′; and *Ccnd3* = forward, 5′-GGAGGTGTGTGAGGAGCAG-3′ and *Ccnd3* = reverse, 5′-CCAGGTAGTTCATAGCCAGAGG-3′.

Statistical Analysis

The Student *t*-test or one-way ANOVA with Bonferonni post hoc analysis was performed using SigmaStat software (SPSS Inc., Chicago, IL). A P value < 0.05 was considered to be statistically significant.

RESULTS

Effect of Akt1 *Null Mutation on Female Fertility*

When *Akt1*$^{-/-}$ female mice were mated to *Akt1*$^{+/+}$ males of proven fertility, we observed the *Akt1*$^{-/-}$ females to be significantly less fertile relative to their *Akt1*$^{+/+}$ female counterparts ($P < 0.05$) (Table 1). This subfertility included both a reduction in the overall number of litters and the number of pups per litter in the *Akt1*$^{-/-}$ females (Table 1). The average number of litters per month for *Akt1*$^{+/+}$ females bred with *Akt1*$^{+/+}$ males was 0.64 ± 0.1 (n = 5), and for *Akt1*$^{-/-}$ females bred to *Akt1*$^{+/+}$ males, the average number of litters per month was 0.11 ± 0.1 (n = 8). The number of pups per litter was significantly reduced in *Akt1*$^{-/-}$ female mice compared to *Akt1*$^{+/+}$ female mice, with 3.6 ± 0.8 pups per litter (n = 8) and 5.8 ± 0.5 pups per litter (n = 5), respectively (Table 1). The average maternal age for production of the first litter for *Akt1*$^{+/+}$ and *Akt1*$^{-/-}$ females was 56 ± 5 days and 100 ± 7 days, respectively ($P < 0.001$).

Comparison of Akt1$^{+/+}$, Akt1$^{+/-}$, *and* Akt1$^{-/-}$ *Female Body and Ovarian Weights*

To characterize the female reproductive physiology of the *Akt1*$^{-/-}$ female mice, body weights and ovarian weights were compared with those of *Akt1*$^{+/+}$ females at PNDs 25, 56, and 90 (Table 2). At all time points examined, significant decreases in the body weights of the *Akt1*$^{-/-}$ mice were observed compared with that of *Akt1*$^{+/+}$ female mice. At PND56, *Akt1*$^{-/-}$ female mice exhibited an approximate 20% decrease in body weight, and, at PND90, there was a 12% decrease in body weight relative to *Akt1*$^{+/+}$ counterparts. Similar to body weight, there was a significant decrease in ovarian weights in the *Akt1*$^{-/-}$ mice at both PND56 and PND90 (Table 2). Ovarian weights at PND25 were reduced by 27.4% relative to *Akt1*$^{+/+}$ mice, and, at PND90, ovarian weights were reduced by 20.6% in *Akt1*$^{-/-}$ mice relative to the *Akt1*$^{+/+}$ littermates. However, when adjusted for ovarian weight relative to body size (i.e., absolute ovarian weight), no differences were observed in *Akt1*$^{+/+}$ and *Akt1*$^{-/-}$ females (Table 2).

Effect of Akt1 *Null Mutation on Sexual Maturity*

Due to the significant decrease in body size of the *Akt1*$^{-/-}$ mice, we determined if there was a delay in sexual maturity in the *Akt1*$^{-/-}$ females by assessing the effect of *Akt1* deletion on the age at pubertal onset and estrous cyclicity. As shown in Table 1, vaginal opening was not significantly delayed in *Akt1*$^{-/-}$ females (PND33.2 ± 1.4; n = 10) when compared with *Akt1*$^{+/+}$ females (PND33.0 ± 1.5; n = 4). However, sexual maturity, as determined by first proestrus, was significantly delayed in *Akt1*$^{-/-}$ females (PND44.8 ± 0.6) compared with *Akt1*$^{+/+}$ females (PND39.8 ± 1.1; n = 3), and the maternal age at first litter was significantly higher in *Akt1*$^{-/-}$ females relative to *Akt1*$^{+/+}$ counterparts (100 ± 7.2 vs. 56 ± 5 days, respectively).

Extension of the Diestrous Cycle in Mature Akt1$^{-/-}$ *Female Mice*

Due to the later age at first proestrus and the later maternal age for first litter in the *Akt1*$^{-/-}$ mice, we examined the length of the estrous cycle of both *Akt1*$^{+/+}$ female mice and *Akt1*$^{-/-}$ female mice at PND90. This age was examined because live litters are observed at this time in *Akt1*$^{-/-}$ females. At PND90,

TABLE 3. Serum hormone levels in *Akt1*$^{+/+}$, *Akt1*$^{+/-}$, and *Akt1*$^{-/-}$ mice at PND50.[a]

Hormone	*Akt1*$^{+/+}$[b,c]	*Akt1*$^{+/-}$[c]	*Akt1*$^{-/-}$[b,c]
FSH (ng/ml)	8.0 ± 1.6 (N = 6)	7.32 ± 1.3 (N = 6)	4.8 ± 1.1 (N = 8)
Estradiol (pg/ml)	7.0 ± 3.2 (N = 33)	ND	12.2 ± 3.0* N = 15
Progesterone (ng/ml)	3.0 ± 0.8 (N = 12)	ND	1.1 ± 0.1* (N = 18)
LH (ng/ml)	0.25 ± 0.04 (N = 11)	0.38 ± 0.15 (N = 6)	0.91 ± 0.3* (N = 8)
Inhibin A (pg/ml)	99.8 ± 21.8 (N = 4)	105.9 ± 27.0 (N = 6)	114.0 ± 19.6 (N = 8)
Inhibin B (pg/ml)	57.4 ± 16.6 (N = 8)	50.5 ± 9.8 (N = 9)	33.5 ± 11.0 (N = 8)

[a] Values represent the mean ± SEM; ND, not determined.
[b] For the statistical analyses of two genotypes (*Akt1*$^{+/+}$ versus *Akt1*$^{-/-}$), a Student *t*-test was used ($P < 0.05$).
[c] For the statistical analyses of all three genotypes, one-way ANOVA was utilized ($P < 0.05$).
* Significant differences in a specific serum hormone observed between *Akt1*$^{+/+}$ and *Akt1*$^{-/-}$ animals.

Akt1$^{-/-}$ females displayed abnormal cycling patterns, although the average cycle length was similar in *Akt*$^{+/+}$, *Akt1*$^{+/-}$, and *Akt1*$^{-/-}$ mice (4.5 ± 0.2 days). Analysis of the estrous cycle profiles in *Akt1*$^{-/-}$ female mice and *Akt1*$^{+/+}$ control mice did reveal a significantly longer diestrus phase in *Akt1*$^{-/-}$ females of approximately 1.5 days longer in duration relative to *Akt1*$^{+/+}$ female mice ($P < 0.05$) (Fig. 1).

Effect of Akt1 *Null Mutation on Follicle Development in Mice at PND25*

To determine the effect of *Akt1* deletion on folliculogenesis, we performed histological and morphometric analyses of follicle numbers at PND25, and compared them between *Akt1*$^{+/+}$ and *Akt1*$^{-/-}$ mice. As expected, *Akt1*$^{+/+}$ females revealed follicles at all developmental stages (primordial, primary, secondary, and antral follicles) and corpora lutea (Fig. 2A). In contrast, the ovaries of *Akt1*$^{-/-}$ mice contained fewer antral follicles compared with *Akt1*$^{+/+}$ controls. In *Akt1*$^{-/-}$ ovaries, we observed follicles with multiple oocytes, as depicted in Figure 2B (dashed circle). Only once did we observe *Akt1*$^{+/+}$ females with more than one oocyte per follicle. The increase in multiple oocytes per follicle may indicate a defect in cyst breakdown in the Akt1$^{-/-}$ ovary. Figure 2C shows follicle numbers at PND25 for both *Akt1*$^{+/+}$ and *Akt1*$^{-/-}$ animals. The number of primordial and primary follicles was not significantly different in *Akt1*$^{-/-}$ ovaries when compared to *Akt1*$^{+/+}$ ovaries; however, the number of preantral follicles in *Akt1*$^{-/-}$ mice was significantly lower than in *Akt1*$^{+/+}$ ovaries, as was the number of antral and mature Graafian follicles (Fig. 2C), with a 2-fold increase in the number of atretic follicles with degenerate oocytes (Fig. 2C).

Effect of Akt1 *Null Mutation on Oocyte Size*

Unexpectedly, we found the diameters of both primary and secondary oocytes to be larger in *Akt1*$^{-/-}$ mice. Primary oocytes were found to have an average diameter of 27.9 ± 1.0 μm versus 22.4 ± 1.0 μm in *Akt1*$^{+/+}$ female primary oocytes. Secondary oocyte diameters were found to be 50.0 ± 1.0 μm in *Akt1*$^{+/+}$ and 53.0 ± 1.0 μm in *Akt1*$^{-/-}$ ovaries.

Responsiveness of PND25 Akt1 *Null Mutant Mice to Exogenous Gonadotropins*

Due to the decrease in the number of mature follicles in *Akt1*$^{-/-}$ mice, we examined whether *Akt1* is involved in the maturation process of follicles by comparing the number of total mature follicles in immature mice after eCG/hCG treatment. As shown in Figure 3C, the number of secondary follicles in the ovaries of *Akt1*$^{-/-}$ mice after eCG/hCG treatment was 2-fold higher than that of *Akt1*$^{+/+}$ mice; however, fewer mature follicles were observed, suggesting that follicular maturation is indeed impaired in *Akt1*$^{-/-}$ mice.

Effect of Akt1 *Null Mutation on Ovarian Steroid Synthesis in Female Mice at PND50*

Both the inability to obtain a significant number of fertile *Akt1*$^{-/-}$ females and the decrease in the number of preantral and antral follicles in the *Akt1*$^{-/-}$ females led us to examine the levels of FSH, estradiol, progesterone, and LH in the serum of these mice at PND50. As depicted in Table 3 at PND50, *Akt1*$^{-/-}$ mice showed a trend for lower levels of FSH. FSH levels in *Akt1*$^{+/+}$ mice were 8.0 ± 1.6 ng/ml (n = 6) and 7.32 + 1.3 ng/ml (n = 6) in *Akt1*$^{+/-}$ mice versus 4.8 ± 1.1 ng/ml (n = 8) in *Akt1*$^{-/-}$ females. Estradiol levels were found to be elevated in

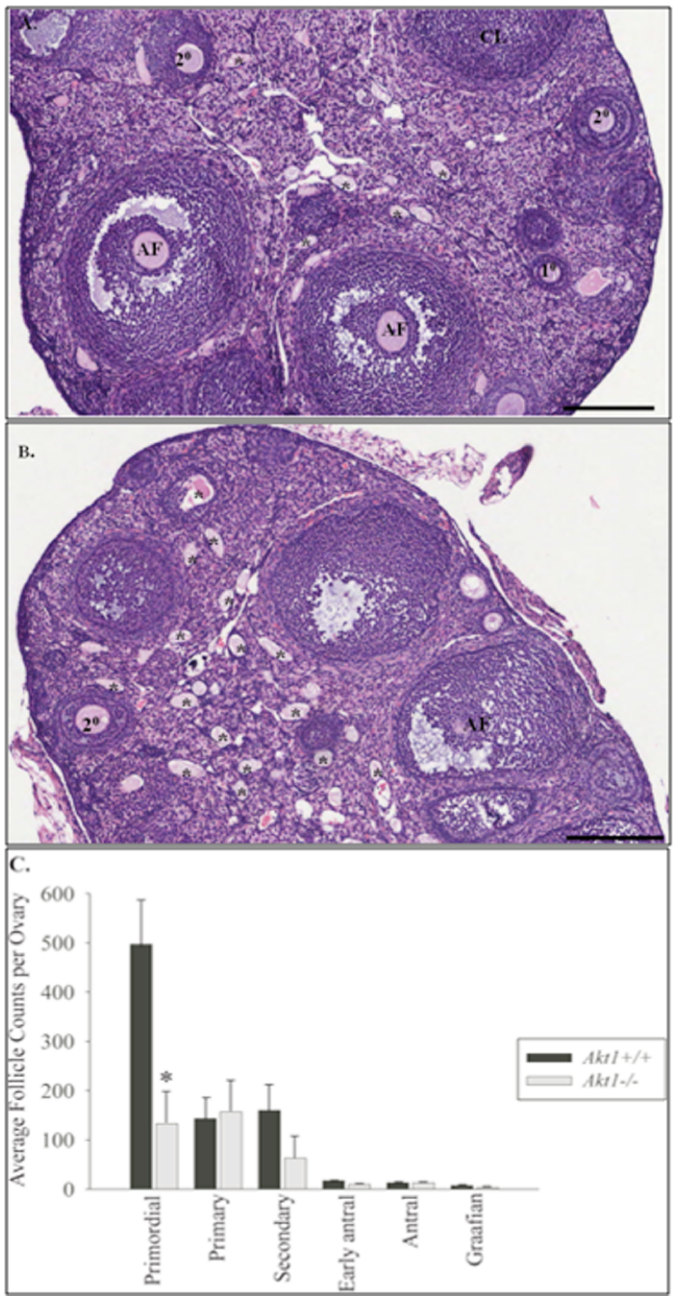

FIG. 4. Effect of *Akt1* null mutation on the primordial follicle pool at PND90. **A**) *Akt1*$^{+/+}$ ovary at PND90. **B**) *Akt*1$^{-/-}$ ovary at PND90. **C**) Follicle counts of *Akt1*$^{+/+}$ and *Akt1*$^{-/-}$ females at PND90 ($n = 3$). The number of primordial (PF), primary (1^0), secondary (2^0), early antral (EAF), antral (AF), and mature Graafian follicles (GF) were determined in *Akt1*$^{+/+}$ and *Akt1*$^{-/-}$ at PND90. Ovaries were serially sectioned, every 10th section was counted, and the total follicle numbers were determined. The total numbers of primordial, primary, secondary, early antral, antral, and mature follicles were multiplied by a factor of 10 to obtain an estimate of the total number of follicles per ovary. These data represent the mean ± SEM of combined results from the analysis of three mice per age group ($P < 0.05$). Asterisk indicates significant difference in primordial follicle number observed between *Akt1*$^{+/+}$ and *Akt1*$^{-/-}$ animals; bar = 200 μm.

Akt1$^{-/-}$ mice (12.2 + 3.0 pg/ml) relative to *Akt1*$^{+/+}$ mice (7.0 ± 3.2 pg/ml). Significantly higher levels of LH were found in *Akt1*$^{-/-}$ females at PND50, with serum levels of 0.91 ± 0.3 ng/ml (n = 8) versus 0.25 ± 0.04 ng/ml (n = 11) in *Akt1*$^{+/+}$ female mice and 0.38 ± 0.15 ng/ml (n = 6) in *Akt1*$^{+/-}$ female mice. Progesterone levels were found to be lower in *Akt1*$^{-/-}$ females

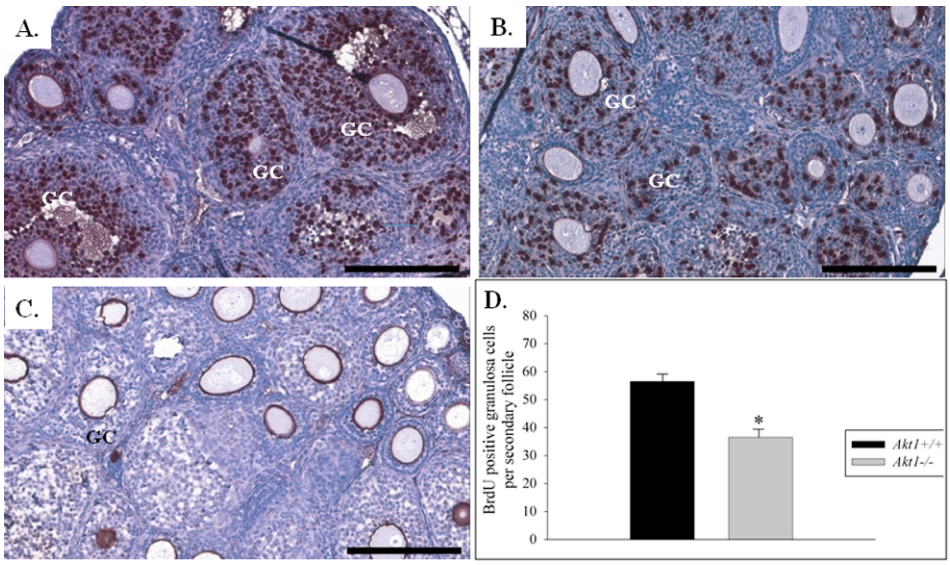

FIG. 5. Effect of *Akt1* null mutation on granulosa cell proliferation in vivo at PND25. Immunohistochemical detection of BrdU incorporation into the nuclei of secondary follicular granulosa cells in 25-day-old $Akt1^{+/+}$ ovary (**A**) and $Akt1^{-/-}$ ovary (**B**). Mice were stimulated with 5 IU ECG for 24 h. **C**) Negative control with primary antibody omitted. **D**) Quantification of percent positive nuclei in secondary follicles in the ovary. GC denotes granulosa cells in the follicles. Average values from two independent experiments are presented; error bars indicate SEM. Statistically significant differences between $Akt1^{-/-}$ mice and matched controls are indicated with asterisks ($P < 0.05$); bar = 200 μm.

(1.1 + 0.1 ng/ml) (n = 18) relative to $Akt1^{+/+}$ females (3.0 ± 0.8 ng/ml) (n = 12). Interestingly, there was a trend toward higher inhibin A levels at PND50 in the $Akt1^{-/-}$ mice than in the $Akt1^{+/+}$ mice (114 pg/ml ± 19.5 [n = 8] versus 99.8 ± 21.8 pg/ml [n = 4], respectively), and there was a trend toward reduced inhibin B serum levels in the $Akt1^{-/-}$ mice relative to $Akt1^{+/+}$ mice (33.5 ± 11.0 pg/ml [n = 8] versus 57.4 ± 16.6 pg/ml [n = 8], respectively).

Analysis of Estradiol and Progesterone in Akt1$^{-/-}$ *Females at PND90*

Because $Akt1^{-/-}$ females are capable of delivering pups to term, we examined the levels of estradiol and progesterone at PND90. We found both estradiol and progesterone levels to be similar in both $Akt1^{-/-}$ and $Akt1^{+/+}$ ovaries at this time point (Table 4). It should be noted that, on several occasions, we observed that $Akt1^{-/-}$ females exhibit weight gain as if pregnant with no pups delivered, suggest-ing that AKT1 may serve other functions in female reproduction, including placentation, parturition, and/or lactation.

Folliculogenesis in Akt1$^{-/-}$ *Females at PND90*

To determine the effect of *Akt1* deletion on folliculogenesis at PND90, we performed histological and morphometric analyses of follicle numbers and compared them between $Akt1^{+/+}$ mice (Fig. 4A) and $Akt1^{-/-}$ mice (Fig. 4B). Both $Akt1^{+/+}$ and $Akt1^{-/-}$ females revealed follicles at all developmental stages (primordial, primary, secondary, and antral follicles) and corpora lutea (Fig. 4, A and C). In contrast, the ovaries of $Akt1^{-/-}$ mice contained significantly fewer primordial follicles compared with $Akt1^{+/+}$ controls (Fig. 4, B and C). The number of primary and secondary follicles was not significantly different in $Akt1^{-/-}$ ovaries when compared to $Akt1^{+/+}$ ovaries. Mature Graafian follicles were observed in both genotypes; however, fewer Graafian follicles were observed in the $Akt1^{-/-}$ ovaries.

TABLE 4. Serum hormone profiles of $Akt1^{+/+}$ and $Akt1^{-/-}$ females at PND90.[a]

Hormone	$Akt1^{+/+}$	$Akt1^{-/-}$
Progesterone (ng/ml)	3.1 ± 0.8 (N = 5)	3.8 ± 1.0 (N = 4)
Estradiol (pg/ml)	6.2 ± 1.2 (N = 4)	7.0 ± 1.2 (N = 5)

[a] Values represent the mean ± SEM; statistical analyses were conducted using Student *t*-test ($P < 0.05$).

Effect of Akt1 *Null Mutation on Granulosa Cell Proliferation In Vivo*

To better understand the cellular basis of the observed folliculogenesis defects in the $Akt1^{-/-}$ ovaries, we assessed the proliferation of granulosa cells in the presence versus absence of *Akt1*. BrdU incorporation in vivo was utilized to directly label granulosa cells in the S phase of the cell cycle and measure granulosa cell proliferation. At 24 h prior to BrdU labeling, matched 21-day-old $Akt1^{+/+}$ and $Akt1^{-/-}$ female mice were stimulated with a single injection of eCG to stimulate proliferation of follicular granulosa cells. Ovaries were harvested the next day following 1 h in vivo BrdU treatment, and ovary sections generated from these mice were labeled with an anti-BrdU antibody. BrdU incorporation was readily detectable in granulosa cells derived from both $Akt1^{+/+}$ mice (Fig. 5A) and $Akt1^{-/-}$ mice (Fig. 5B). However, there was a reduction in the number of positively stained granulosa cells labeled with BrdU in the $Akt1^{-/-}$ ovaries in response to hormonal treatment (Fig. 5C).

Neither Akt2 *nor* Akt3 *Compensate for* Akt1 *Deficiency at the mRNA or Protein Level*

Although the *Akt* gene family is implicated in a survival response to genotoxic injury in multiple cell types, it is not known to what degree there is functional overlap between these family members in the ovary. We first examined the activation of *Akt* in the ovary at PND50, and found decreased phosphorylation at the threonine 308 site in $Akt1^{-/-}$ ovaries (Fig. 6A), but not at Ser473 (Fig. 6A). Next, we examined both the level of *Akt*2 and *Akt*3 mRNA and protein in $Akt1^{+/+}$ and $Akt1^{-/-}$ ovaries at PND50. We found similar levels of expression for *Akt*2 mRNA (Fig. 6B) and protein (Fig. 6A) in both $Akt1^{+/+}$ and $Akt1^{-/-}$ mice. There was a trend toward reduced *Akt*3 mRNA expression in the $Akt1^{-/-}$ ovaries (Fig. 6C) relative to $Akt1^{+/+}$ ovaries, suggesting that *Akt*3 may contribute to the $Akt1^{-/-}$ phenotype. However, we did not observe a decrease in *Akt3* at the protein level (Fig. 6A).

Kitl *and* Bcl2l1 *Are Significantly Reduced in* Akt1$^{-/-}$ *Ovaries*

Kitl plays a role in oocyte growth, survival, and maturation [27]. Therefore, we examined the level of *Kitl* mRNA in both *Akt1*$^{+/+}$ and *Akt1*$^{-/-}$ ovaries. There was a 2-fold reduction in the levels of *Kitl* mRNA in *Akt1*$^{-/-}$ ovaries relative to *Akt1*$^{+/+}$ ovaries (Fig. 7A). Because of the role of *Kitl* in granulosa cell survival and protection of the oocyte, we examined *Bcl2l1* (Fig. 7B), an antiapoptotic factor and well-known downstream target of the AKT1 signaling pathway [28]. Again, we found significantly reduced levels of *Bcl2l1* in the *Akt1*$^{-/-}$ ovaries, suggesting that the PIK3/AKT1 signaling pathway plays a role in folliculogenesis.

Localization Patterns and Decreased mRNA Expression of Members of the Cyclin D Family in Akt1$^{+/+}$ *and* Akt1$^{-/-}$ *Ovaries*

Due to the decreased proliferative rates of the granulosa cells, as measured by BrdU labeling in the secondary follicles of *Akt1*$^{-/-}$ ovaries, we examined the expression levels of *Ccnd1*, *Ccnd2*, and *Ccnd3* (Fig. 7, C–E). Members of the cyclin D family are implicated in the regulation of proliferation of granulosa cells [29, 30]. We found that *Ccnd3* mRNA expression levels (Fig. 7E) were reduced 3-fold in the *Akt1*$^{-/-}$ ovary relative to the *Akt1*$^{+/+}$ ovary, and that there was a 2-fold reduction in *Ccnd1* mRNA expression levels (Fig. 7C) as well, although it did not reach statistical significance. Importantly, *Ccnd2* mRNA expression levels (Fig. 7D) remained the same in both *Akt1*$^{+/+}$ and *Akt1*$^{-/-}$ animals.

To localize *Ccnd1*, *Ccnd2*, and *Ccnd3* to particular cells within the ovary, ovaries were examined at PND50 by immunohistochemistry. *Ccnd1* staining was found to be relatively weak in the ovary, with minimal staining detected in thecal cells of both *Akt1*$^{+/+}$ (Fig. 8A, arrows) and *Akt1*$^{-/-}$ ovaries (Fig. 8D, arrow). Staining of *Ccnd1* did appear less intense in the *Akt1*$^{-/-}$ ovary. We also observed weak cytoplasmic staining of Ccnd1 in the primordial follicles (Fig. 8D, bracket). As a positive control, oviduct stained positive for *Ccnd1* within the same ovarian tissue sections examined (Fig. 8I). *Ccnd2* expression was localized primarily to the cytoplasm of granulosa cells in both the *Akt1*$^{+/+}$ (Fig. 8B) and *Akt1*$^{-/-}$ (Fig. 8E) ovaries. *Ccnd3* localized to the nuclei of primordial (Fig. 8, C and F, asterisks) and primary follicles (Fig. 8, C and F, arrows) in both *Akt1*$^{+/+}$ (Fig. 8C) and *Akt1*$^{-/-}$ ovaries (Fig. 8F).

DISCUSSION

Numerous studies have shown a role for the deletion of *Akt1* in mice to lead to decreases in both cell proliferation and apoptosis [9–19]. However, the role of *Akt1* in female reproductive tissues remains uncharacterized. Our results show that *Akt1* deletion leads to POF. The extreme subfertility that *Akt1*$^{-/-}$ female mice exhibit appears to arise from altered hormonal signals, as exemplified by a delay in the first estrous cycle and an extension of the diestrous phase in *Akt1*$^{-/-}$ females. The ovaries of *Akt1*$^{-/-}$ female mice also exhibit abnormal gene expression of two of the cyclin D family members, *Ccnd1* and *Ccnd3*, and reduced levels of expression of the survival factors, *Kitl* and *Bcl2l1*, resulting in decreased granulosa cell proliferation in vivo. Moreover, by PND90, there is a dramatic decrease in the number of primordial follicles in *Akt1*$^{-/-}$ female mice, indicating POF.

Previous studies have demonstrated that an adequate mass of adipose tissue is required for proper onset of puberty and fertility, suggesting an important link between energy homeostasis and reproductive function [31]. Because *Akt1*$^{-/-}$ mice exhibit a smaller body size throughout their lifetime, we examined the onset of puberty in *Akt1*$^{+/+}$ and *Akt1*$^{-/-}$ mice. We found no difference in the timing of vaginal opening, but we did observe a difference in the timing of the first proestrus, with a delay of approximately 5 days in *Akt1*$^{-/-}$ females. No difference in the absolute ovarian weights of *Akt1*$^{+/+}$ or *Akt1*$^{-/-}$ mice was found at PND25, suggesting that the small

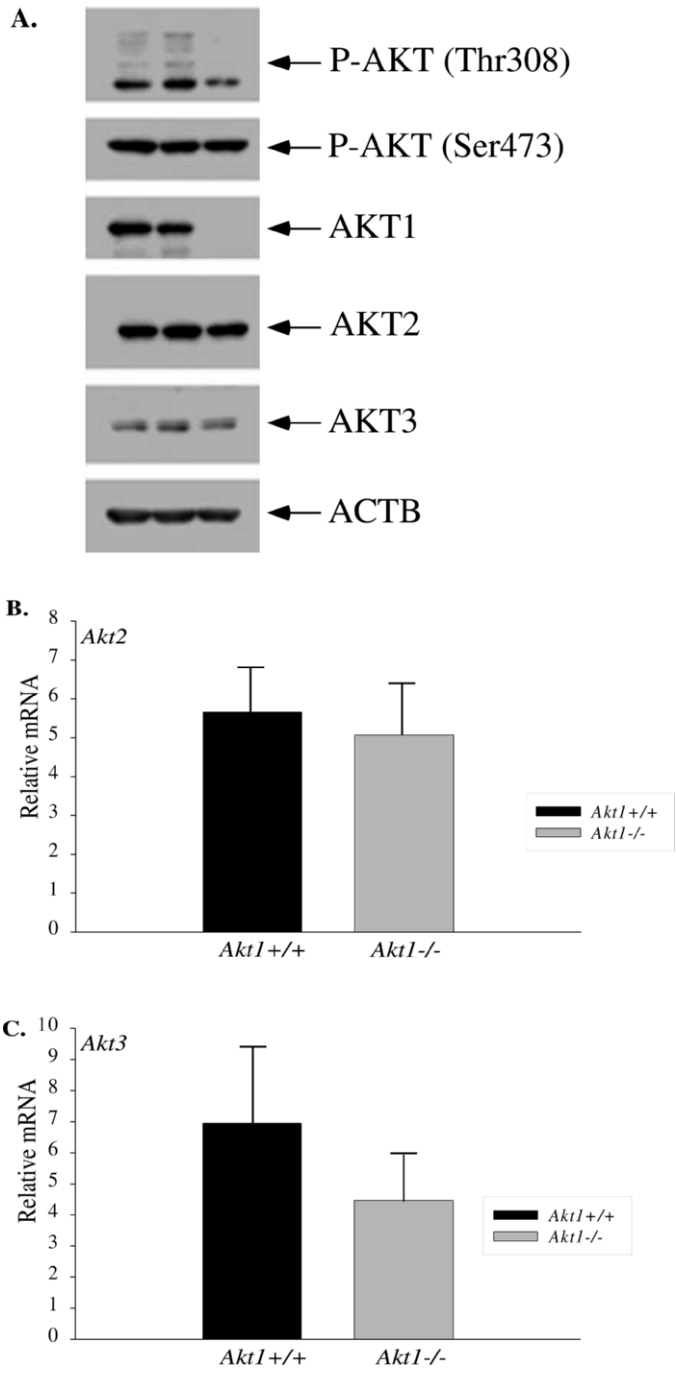

FIG. 6. Neither *Akt2* nor *Akt3* compensates for *Akt1*$^{-/-}$ at the mRNA or protein level at PND50. **A**) Representative Western blots of *Akt1*$^{+/+}$, *Akt1*$^{+/-}$, and *Akt1*$^{-/-}$ ovaries at PND50. Shown are phosphorylated Ser^{473} AKT and Thr^{308} AKT1, and AKT1, AKT2, and AKT3 total protein; β-actin was used as a loading control. Changes in the relative mRNA expression of *Akt2* (**B**) and of *Akt3* (**C**) in *Akt1*$^{-/-}$ (gray bars) ovaries relative to *Akt1*$^{+/+}$ (black bars) control ovaries. Expression was determined by using the Pfaffl method.

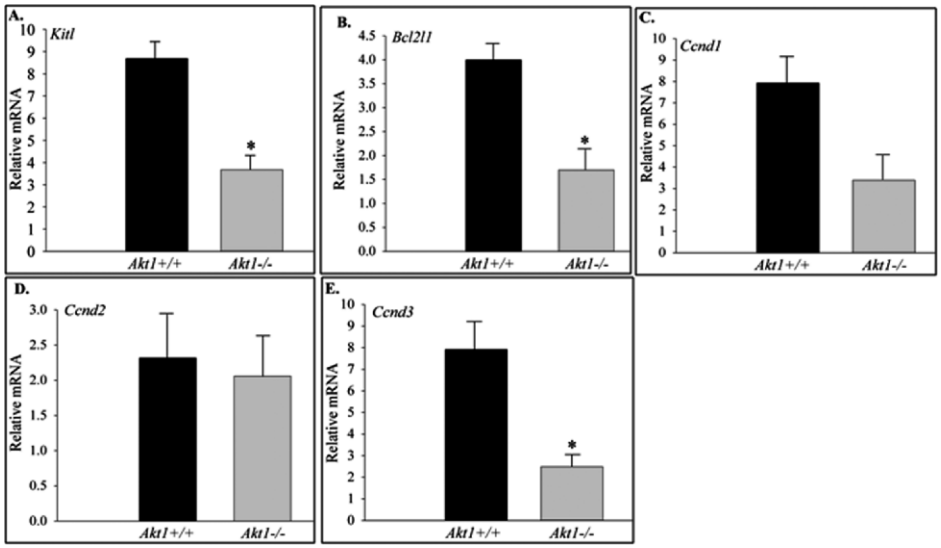

FIG. 7. Reduced levels of *Kitl*, *Ccnd3*, and *Bcl2l1* in $Akt1^{-/-}$ mouse ovaries at the mRNA level at PND50. Changes in the relative mRNA expression of *Kitl* (**A**), *Bcl2l1* (**B**), *Ccnd1* (**C**), *Ccnd2* (**D**), and *Ccnd3* (**E**) are depicted in graphic form in $Akt1^{+/+}$ (black bars) and $Akt1^{-/-}$ (gray bars) ovaries. Expression was determined by using the Pfaffl method. The data are shown as means ± the SEM. Significance was determined by ANOVA; $^{*}P < 0.05$.

body size phenotype of the $Akt1^{-/-}$ female is not the sole reason for the extreme female subfertility in these mice.

At PND50, $Akt1^{-/-}$ animals exhibit higher LH levels. This finding suggests that the trigger to signal ovulation is present in the $Akt1^{-/-}$ mice; however, the significant decrease in preantral and antral follicle formation in the $Akt1^{-/-}$ animals and the increased number of degenerate oocytes indicates an aberrant response to this LH signal. Chronically elevated LH levels have been reported to deplete the primordial follicle pool, which hastens the onset of reproductive senescence [32]. In agreement with this, by PND90, we observed a significant reduction in the number of primordial follicles in the $Akt1^{-/-}$ ovaries, suggesting accelerated depletion of the primordial follicle pool. In addition to the higher LH levels, we also observed a trend toward higher inhibin A serum levels and a reduction in inhibin B serum levels in the $Akt1^{-/-}$ ovaries. In women, inhibin A is a marker of dominant follicle and corpus

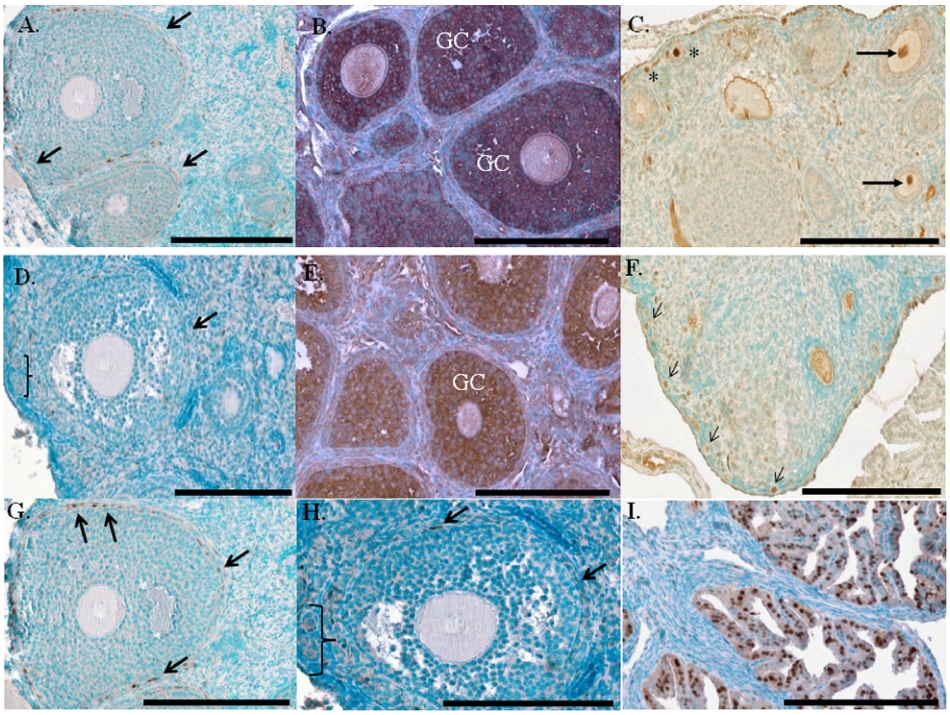

FIG. 8. Localization of *Ccnd1*, *Ccnd2*, and *CCnd3* Family members in $Akt1^{+/+}$ and $Akt1^{-/-}$ ovaries at PND50. CCND1, CCND2, and CCND3 protein were analyzed by immunohistochemistry. Immunodetection of CCND1 in $Akt1^{+/+}$ (**A**) and $Akt1^{-/-}$ (**D**) ovaries, and immunodetection of CCND1 in the oviduct (**I**). Weak positive staining for CCND1 is observed in the thecal cells of both genotypes (**A** and **D**, arrows). Immunodetection of CCND2 in $Akt1^{+/+}$ (**B**) and $Akt1^{-/-}$ (**E**) ovaries. Positive staining, as indicated by diaminobenzidine signal (brown staining), for CCND2 is observed in granulosa cells (GC) of both genotypes (**B** and **E**). Immunodetection of CCND3 in $Akt1^{+/+}$ (**C**) and $Akt1^{-/-}$ (**F**) ovaries. Positive staining is observed in the nuclei of oocytes from primordial (**C** and **F**, asterisks) and primary follicles (**C** and **F**, arrows). **G**) Higher magnification of nuclear staining for CCND1 in $Akt1^{+/+}$ follicle (**A**), which can be observed around the perimeter of the follicle (arrows). **H**) Higher magnification of nuclear staining for CCND1 in $Akt1^{-/-}$ follicle (**D**), which can be observed around the perimeter of follicle (arrows). Cytoplasmic staining for CCND1 is also observed in primordial follicles (bracket). **I**) Strong nuclear staining for CCND1 is observed in the oviduct; bar = 200 μm.

luteum activity, and decreases in inhibin A are associated with polycystic ovary syndrome [33].

Besides changes in gonadotropin levels, the reduced numbers of growing follicles in $Akt1^{-/-}$ ovaries prompted us to examine the proliferative potential of the granulosa cells in the $Akt1^{-/-}$ mice. We reasoned that the decreased fertility may be due, in part, to defective follicle growth due to reduced granulosa cell proliferation and/or an increase in atretic follicles. Indeed, we observed decreased granulosa cell proliferation as evidenced by decreased incorporation of BrdU in the follicles of $Akt1^{-/-}$ mice. Moreover, we observed decreased expression levels of *Kitl*, which is expressed primarily in granulosa cells. *Kitl*, along with *c-Kit*, protects preantral follicles from apoptosis [34, 35]. *Ccnd3* expression, which regulates G1/S-phase progression, was also reduced in the $Akt1^{-/-}$ ovaries; however, *Ccnd2* levels remained fairly constant in both $Akt1^{+/+}$ and $Akt1^{-/-}$ ovaries. This is in contrast to a recent report in which *Ccnd1* levels were regulated by an *Akt*1-dependent pathway [36]. *Bcl2l1* expression, an established downstream target of the PIK/3AKT1 signaling pathway, was also reduced. Importantly, *Bcl2l1* has been shown to play a protective role in rat primordial oocyte survival in vitro by regulating BAX expression levels [37]. It should be noted, however, that mRNA expression was measured in whole-ovary extract, and not isolated cell types. Use of the whole-ovary extract in our studies may mask changes in a specific cell type.

Several features of our current study with respect to oocyte development also merit attention. The incidence of multioocyte follicles appeared to be unique to the $Akt1^{-/-}$ ovary, because they were extremely rare or not present in the $Akt1^{+/+}$ or $Akt1^{+/-}$ ovaries. This type of abnormal follicle has also been noted in ovaries of mutant mice lacking *Gdf9* or *Bmp15*, both of which are oocyte-secreted growth factors [38, 39]. Several other deletions of genes expressed in granulosa cells also exhibit this aberration, as in ovaries of mice lacking the *Nr0b1* (previous symbol, *Ahch*) gene [40], which encodes the transcription factor, DAX1, involved in sex determination, or the Ca^{2+}/calmodulin-dependent protein kinase IV knockout females that show reduced fertility [41], and in mice that overexpress the inhibin alpha gene [42]. Although the mechanisms underlying such abnormalities are complex, it is possible that early developmental events that lead to follicle organization are aberrant and/or incomplete in the $Akt1^{-/-}$ ovary. Moreover, evidence indicates that estrogen signals through multiple pathways to regulate oocyte cyst breakdown and primordial follicle assembly in the neonatal mouse ovary [43]. Indeed, we did observe both follicles with multiple oocytes per follicle and higher estradiol levels in the $Akt1^{-/-}$ ovary.

Another intriguing observation was the increase in the size (diameter) of the primary and secondary oocytes in the $Akt1^{-/-}$ mice relative to $Akt1^{+/+}$ mice and the increase in the number of degenerate oocytes. Although not statistically significant, we did observe reduced serum levels of FSH in PND50 $Akt1^{-/-}$ females compared with $Akt1^{+/+}$ and $Akt1^{+/-}$ animals. Previous work has indicated that microinjection of a myristolated form of *Akt* in mouse oocytes leads to in vitro meiotic maturation, and this effect requires cGMP-inhibited cAMP phosphodiesterase 3A [44]. Moreover, the activation of *Akt* stimulates the metaphase I-to-metaphase II transition in bovine oocytes [45]; and the PIK3/AKT pathway has been shown to participate in the FSH-induced meiotic maturation of both mouse and *Xenopus* oocytes [46, 47]. Perhaps, the majority of oocytes of the $Akt1^{-/-}$ female fail to undergo FSH-induced meiotic maturation, resulting in degenerate oocytes and subsequent infertility.

In conclusion, we propose a role for the PTEN/PIK3/AKT1 signaling pathway that promotes healthy oocyte development and folliculogenesis. We propose that the communication between granulosa cells and oocyte is altered, leading to an increase in the size of primary and secondary oocytes in the $Akt1^{-/-}$ animals. Therefore, *Akt1* is critical for the proper growth and maturation of both the oocyte and granulosa cells. The loss of *Akt1* leads to miscommunication between oocyte and granulosa cells, resulting in degenerate oocytes and POF. This significant but incomplete disruption in female fertility is not likely due to compensation by other *PKB*/AKT family members, but factors yet to be identified. *PKBα*/AKT1 is instrumental in the precise timing of the female reproductive lifespan. We believe that these phenomena may have relevance to POF and lower reproductive success in middle-aged women. Further studies on the functions of *Akt1* and its family members in the ovary can be expected to advance the understanding of the molecular mechanisms of female infertility.

ACKNOWLEDGMENT

We would like to thank the Freiman laboratory for critical reading of the manuscript.

REFERENCES

1. McGee EA, Hsueh AJ. Initial and cyclic recruitment of ovarian follicles. Endocr Rev 2000; 21:200–214.
2. Picton HM. Activation of follicle development: the primordial follicle. Theriogenology 2001; 55:1193–1210.
3. Hillier SG. Gonadotropic control of ovarian follicular growth and development. Mol Cell Endocrinol 2001; 179:39–46.
4. Howles CM. Role of LH and FSH in ovarian function. Mol Cell Endocrinol 2000; 161:25–30.
5. Fortune JE. The early stages of follicular development: activation of primordial follicles and growth of preantral follicles. Anim Reprod Sci 2003; 78:135–163.
6. Reddy P, Liu L, Adhikari D, Jagarlamudi K, Rajareddy S, Shen Y, Du C, Tang W, Hämäläinen T, Peng SL, Lan ZJ, Cooney AJ, et al. Oocyte-specific deletion of Pten causes premature activation of the primordial follicle pool. Science 2008; 319:611–613.
7. Reddy P, Adhikari D, Zheng W, Liang S, Hämäläinen T, Tohonen V, Ogawa W, Noda T, Volarevic S, Huhtaniemi I, Liu K. PDK1 signaling in oocytes controls reproductive aging and lifespan by manipulating the survival of primordial follicles. Hum Mol Genet 2009; 18:2813–2824.
8. John GB, Shirley LJ, Gallardo TD, Castrillon DH. Specificity of the requirement for Foxo3 in primordial follicle activation. Reproduction 2007; 133:855–863.
9. Nicholson KM, Anderson NG. The protein kinase B/*Akt* signalling pathway in human malignancy. Cell Signal 2002; 14:381–395.
10. Chen WS, Xu PZ, Gottlob K, Chen ML, Sokol K, Shiyanova T, Roninson I, Weng W, Suzuki R, Tobe K, Kadowaki T, Hay N. Growth retardation and increased apoptosis in mice with homozygous disruption of the *Akt*1 gene. Genes Dev 2002; 15:2203–2208.
11. Cho H, Thorvaldsen JL, Chu Q, Feng F, Birnbaum MJ. *Akt1*/PKBalpha is required for normal growth but dispensable for maintenance of glucose homeostasis in mice. J Biol Chem 2001; 276:38349–38352.
12. Cho H, Mu J, Kim JK, Thorvaldsen JL, Chu Q, Crenshaw EB III, Kaestner KH, Bartolomei MS, Shulman GI, Birnbaum MJ. Insulin resistance and a diabetes mellitus-like syndrome in mice lacking the protein kinase *Akt*2 (PKB beta). Science 2001; 292:1728–1731.
13. Garofalo RS, Orena SJ, Rafidi K, Torchia AJ, Stock JL, Hildebrandt AL, Coskran T, Black SC, Brees DJ, Wicks JR, McNeish JD, Coleman KG. Severe diabetes, age-dependent loss of adipose tissue, and mild growth deficiency in mice lacking *Akt*2/PKB beta. J Clin Invest 2003; 112:197–208.
14. Peng XD, Xu PZ, Chen ML, Hahn-Windgassen A, Skeen J, Jacobs J, Sundararajan D, Chen WS, Crawford SE, Coleman KG, Hay N. Dwarfism, impaired skin development, skeletal muscle atrophy, delayed bone development, and impeded adipogenesis in mice lacking *Akt*1 and *Akt*2. Genes Dev 2003; 17:1352–1365.
15. Yang ZZ, Tschopp O, Di-Poï N, Bruder E, Baudry A, Dümmler B, Wahli W, Hemmings BA. Dosage-dependent effects of *Akt*1/protein kinase B alpha (PKBalpha) and *Akt*3/PKB gamma on thymus, skin, and

cardiovascular and nervous system development in mice. Mol Cell Biol 2005; 25:10407–10418.
16. Easton RM, Cho H, Roovers K, Shineman DW, Mizrahi M, Forman MS, Lee VM, Szabolcs M, de Jong R, Oltersdorf T, Ludwig T, Efstratiadis A, et al. Role for *Akt*3/protein kinase Bgamma in attainment of normal brain size. Mol Cell Biol 2005; 25:1869–1878.
17. Tschopp O, Yang ZZ, Brodbeck D, Dummler BA, Hemmings-Mieszczak M, Watanabe T, Michaelis T, Frahm J, Hemmings BA. Essential role of protein kinase B gamma (PKB gamma/*Akt*3) in postnatal brain development but not in glucose homeostasis. Development 2005; 132: 2943–2954.
18. Rasoulpour T, DiPalma K, Kolvek B, Hixon M. *Akt1* suppresses radiation-induced germ cell apoptosis in vivo. Endocrinology 2006; 147:4213–4221.
19. Rogers R, Ouellet G, Brown C, Moyer B, Rasoulpour T, Hixon M. Cross-talk between the *Akt* and NF-kappaB signaling pathways inhibits MEHP-induced germ cell apoptosis. Toxicol Sci 2008; 106:497–508.
20. Liu K. Stem cell factor (SCF)-kit mediated phosphatidylinositol 3 (PI3) kinase signaling during mammalian oocyte growth and early follicular development. Front Biosci 2006; 11:126–135.
21. Meng C, Shi F, Zhou Z, Huang R, Liu G, Watanabe G, Taya K. Cellular localization of inhibin alpha-subunit, PKB/*Akt* and FoxO3a proteins in the ovaries of minipigs. J Reprod Dev 2007; 53:229–236.
22. Reddy P, Shen L, Ren C, Boman K, Lundin E, Ottander U, Lindgren P, Liu YX, Sun QY, Liu K. Activation of *Akt* (PKB) and suppression of FKHRL1 in mouse and rat oocytes by stem cell factor during follicular activation and development. Dev Biol 2005; 281:160–170.
23. Richards JS, Sharma SC, Falender AE, Lo YH. Expression of FKHR, FKHRL1, and AFX genes in the rodent ovary: evidence for regulation by IGF-I, estrogen, and the gonadotropins. Mol Endocrinol 2002; 16:580–599.
24. Goto M, Iwase A, Ando H, Kurotsuchi S, Harata T, Kikkawa F. PTEN and *Akt* expression during growth of human ovarian follicles. J Assist Reprod Genet 2007; 24:541–546.
25. Pedersen T. Follicle kinetics in the ovary of the cyclic mouse. Acta Endocrinol (Copenh) 1970; 64:304–323.
26. Cooper RL, Goldman JM, Vandenbergh JG. Monitoring of the estrous cycle in the laboratory rodent by vaginal lavage. In: Heindel JJ, Chapin RE (eds.), Methods in Toxicology, vol. 3B. San Diego: Academic Press; 1993: 45–56.
27. Thomas FH, Vanderhyden BC. Oocyte-granulosa cell interactions during mouse follicular development: regulation of kit ligand expression and its role in oocyte growth. Reprod Biol Endocrinol 2006; 4:19.
28. Rucker EB III, Dierisseau P, Wagner KU, Garrett L, Wynshaw-Boris A, Flaws JA, Hennighausen L. Bcl-x and Bax regulate mouse primordial germ cell survival and apoptosis during embryogenesis. Mol Endocrinol 2000; 14:1038–1052.
29. Sicinski P, Donaher JL, Geng Y, Parker SB, Gardner H, Park MY, Robker RL, Richards JS, McGinnis LK, Biggers JD, Eppig JJ, Bronson RT, et al. *Ccnd1* is an FSH-responsive gene involved in gonadal cell proliferation and oncogenesis. Nature 1996; 384:470–474.
30. Robker RL, Richards JS. Hormone-induced proliferation and differentiation of granulosa cells: a coordinated balance of the cell cycle regulators *Ccnd1* and p27Kip1. Mol Endocrinol 1998; 12:924–940.
31. Cameron JL. Nutritional determinants of puberty. Nutr Rev 1996; 54:s17–s22.
32. Flaws JA, Abbud R, Mann RJ, Nilson JH, Hirshfield AN. Chronically elevated luteinizing hormone depletes primordial follicles in the mouse ovary. Biol Reprod 1997; 57:1233–1237.
33. Tsigkou A, Luisi S, Reis FM, Petraglia F. Inhibins as diagnostic markers in human reproduction. Adv Clin Chem 2008; 45:1–29.
34. Vanderhyden BC, Telfer EE, Eppig JJ. Mouse oocytes promote proliferation of granulosa cells from preantral and antral follicles in vitro. Biol Reprod 1992; 46:1196–1200.
35. Packer AI, Hsu YC, Besmer P, Bachvarova RF. The ligand of the c-kit receptor promotes oocyte growth. Dev Biol 1994; 161:194–205.
36. Kayampilly PP, Menon KM. Follicle-stimulating hormone inhibits adenosine 5′-monophosphate-activated protein kinase activation and promotes cell proliferation of primary granulosa cells in culture through an *Akt*-dependent pathway. Endocrinology 2009; 150:929–935.
37. Jin X, Han CS, Yu FQ, Wei P, Hu ZY, Liu YX. Anti-apoptotic action of stem cell factor on oocytes in primordial follicles and its signal transduction. Mol Reprod Dev 2005; 70:82–90.
38. Yan C, Wang P, DeMayo J, DeMayo FJ, Elvin JA, Carino C, Prasad SV, Skinner SS, Dunbar BS, Dube JL, Celeste AJ, Matzuk MM. Synergistic roles of bone morphogenetic protein 15 and growth differentiation factor 9 in ovarian function. Mol Endocrinol 2001; 15:854–866.
39. Galloway SM, Gregan SM, Wilson T, McNatty KP, Juengel JL, Ritvos O, Davis GH. Bmp15 mutations and ovarian function. Mol Cell Endocrinol 2002; 191:15–18.
40. Yu RN, Ito M, Saunders TL, Camper SA, Jameson JL. Role of Ahch in gonadal development and gametogenesis. Nat Genet 1998; 20:353–357.
41. Wu JY, Gonzalez-Robayna IJ, Richards JS, Means AR. Female fertility is reduced in mice lacking Ca^{2+}/calmodulin-dependent protein kinase IV. Endocrinology 2000; 141:4777–4783.
42. McMullen ML, Cho BN, Yates CJ, Mayo KE. Gonadal pathologies in transgenic mice expressing the rat inhibin alpha-subunit. Endocrinology 2001; 142:5005–5014.
43. Chen Y, Jefferson WN, Newbold RR, Padilla-Banks E, Pepling ME. Estradiol, progesterone, and genistein inhibit oocyte nest breakdown and primordial follicle assembly in the neonatal mouse ovary in vitro and in vivo. Endocrinology 2007; 148:3580–3590.
44. Han SJ, Vaccari S, Nedachi T, Andersen CB, Kovacina KS, Roth RA, Conti M. Protein kinase B/*Akt* phosphorylation of PDE3A and its role in mammalian oocyte maturation. EMBO J 2006; 25:5716–5725.
45. Tomek W, Smiljakovic T. Activation of Akt (protein kinase B) stimulates metaphase I to metaphase II transition in bovine oocytes. Reproduction 2005; 130:423–430.
46. Andersen CB, Roth RA, Conti M. Protein kinase B/*Akt* induces resumption of meiosis in *Xenopus* oocytes. J Biol Chem 1998; 273: 18705–18708.
47. Hoshino Y, Yokoo M, Yoshida N, Sasada H, Matsumoto H, Sato E. Phosphatidylinositol 3-kinase and *Akt* participate in the FSH-induced meiotic maturation of mouse oocytes. Mol Reprod Dev 2004; 69:77–86.